

Mechanics of Catalyst Motion during Metal Assisted Chemical Etching of Silicon

Chang Quan Lai¹, He Cheng¹, W. K. Choi^{1,2,3}, Carl V. Thompson^{1,4}*

¹Advanced Materials for Micro- and Nano-Systems Programme, Singapore-MIT Alliance, National University of Singapore, Singapore 117576, Singapore

²Department of Electrical and Computer Engineering, National University of Singapore, Singapore 117576, Singapore

³NUS Graduate School for Integrative Sciences and Engineering, National University of Singapore, Singapore 117456, Singapore

⁴Department of Materials Science and Engineering, MIT, Cambridge, MA 02139, USA.

*Corresponding Author, email: cthomp@mit.edu

Supporting Information

Supporting Information 1: List of important symbols used in this study

Symbols	Meaning
$\{ \}$	Concentration of species enclosed within brackets on the surface of the cathode or anode. Unit: mol/m ²
$[]$	Concentration of species enclosed within brackets in the etching solution. Unit: mol/m ³
t	Time.
I_c	Number of holes generated by the cathode per unit time.
I_a	Number of holes consumed by the anode per unit time.
A_{Au}	Area of the Au taking part in the cathodic reaction.
A_{Si}	Area of the Si taking part in the anodic reaction.
A	Area of a single side of the Au film. Equivalent to the projected area of Si etching.
N_c	Stoichiometric ratio of number of holes to number of H ₂ O ₂ molecules in the cathodic reaction.
N_a	Stoichiometric ratio of number of holes to number of HF molecules in the anodic reaction.
N_h	Stoichiometric ratio of holes to Si in the anodic reaction.
F	Faraday's constant. Equal to 96485 C/mol.
k_c	Rate constant for cathodic reaction.
k_a	Rate constant for anodic reaction.
D_c	Dissociation constant of HF.
s	Defined as etch range in this study. It is the depth that can be etched into

	Si by a stationary catalyst during MACE.
H	Thickness of the Au catalyst.
G	Geometric parameter. Equal to sA_{Au}/A_{Si} .
σ	Van der Waals' forces of attraction per unit area between Si and the catalyst.
C	Hamaker's constant.
b	Width of the Au nanobeam or diameter of holes in the Au film. $b = 315\text{nm}$ in this study.
L	Length of the Au nanobeam. $L = 2\mu\text{m}$ unless stated otherwise.
E	Young's modulus. The value for Au used in this study is 600GPa^1 .
ψ	Second moment of area.
ν	Etch rate.
Q	Amount of charge carried by a single hole. Equal to $1.6 \times 10^{-19}/\text{m}^3$.
χ	Density of atoms in Si. Equal to $5 \times 10^{28}/\text{m}^3$.
ρ	Density of Au. Equal to $19300 \text{ kg}/\text{m}^3$.
β	Bending stress.
β_c	Critical bending stress.
ε	Dielectric constant.
n	Refractive index.
h_0	Planck's constant.
k	Boltzmann's constant.
T	Temperature.
ν_e	Mean absorption frequency ($\approx 3 \times 10^{15} \text{ Hz}$) ³ .

Supporting Information 2: Derivation of expressions for I_c , I_a and s

Assumptions of model:

1. The production of h^+ at the cathode is the rate limiting step.
2. All the h^+ injected into Si is consumed at the solution/Si interfaces near the Au catalyst. This assumption is based on the results reported in reference 6 where the authors made the observation that Si etching away from the Au catalyst is minimal for MACE conditions such as those employed in this study.
3. Charge carrier concentration in Si is insignificant compared to cathodic/ anodic current.
4. The cathodic and anodic reactions only occur at an appreciable rate when Au and Si make electrical contact i.e. they are not charged entities when separated.
5. The Au film is rigid (i.e. does not bend) in the y-axis.

Let us start by considering an etching solution with a bulk concentration of $[H_2O_2]$ and $[HF]$ (in mol/m^3). By making use of the Langmuir isotherm⁴, the surface concentrations (in mol/m^2) of H_2O_2 , $\{H_2O_2\}$, and H^+ , $\{H^+\}$, adsorbed onto the Au surface is

$$\{H_2O_2\} = \{H_2O_2\}_{\max} K_1 [H_2O_2] \text{ ----- (S2.1)}$$

$$\{H^+\} = \{H^+\}_{\max} K_2 [H^+] \text{ ----- (S2.2)}$$

where $\{H_2O_2\}_{\max}$ and $\{H^+\}_{\max}$ refer to the maximum surface concentrations of H_2O_2 and H^+ that can be adsorbed onto the Au surface at a particular temperature respectively. K_1 and K_2 are constants and it has been assumed that $K_1 [H_2O_2] \ll 1$ and $K_2 [H^+] \ll 1$ so that we arrive at eq. (S2.1) and eq. (S2.2). Note that $[H^+]$ can also be expressed in terms of $[HF]$ with the following relation

$$[H^+] = \sqrt{D_c} [HF]^{\frac{1}{2}} \text{ ----- (S2.3)}$$

where D_c refers to the dissociation constant of HF.

The rate equation for the cathodic reaction can be given as⁵

$$-\frac{d\{H_2O_2\}}{dt} = k\{H_2O_2\}^m\{H^+\}^q \text{ ----- (S2.4)}$$

where k is the rate constant, t is time and m and q are constants. By making use of the expressions in eq. (S2.1) – (2.3), eq. (S2.4) can be re-written as

$$-\frac{d\{H_2O_2\}}{dt} = k_c[H_2O_2]^m[HF]^n \text{ ----- (S2.5)}$$

where k_c is a constant and $k_c = k(K_1)^m(K_2)^{2n}(D_c)^n(\{H_2O_2\}_{\max})^m(\{H^+\}_{\max})^{2n}$. Note that $n = q/2$ for the simplification of the notations for eq. (1) in the main text.

From the stoichiometric relation between H_2O_2 and h^+ in the cathodic reaction shown in the main text, the cathodic current I_c can therefore be calculated as

$$I_c = -A_{Au}N_cF\left(-\frac{d\{H_2O_2\}}{dt}\right) = A_{Au}N_cFk_c[H_2O_2]^m[HF]^n \text{ ----- (S2.6)}$$

where A_{Au} is the surface area of the gold-solution interface, N_c is the number of moles of holes produced from one mole of H_2O_2 consumed and F is the Faraday's constant (≈ 96485 C/mol). Note that $N_c = 2$.

Going through the same analysis for the anode, we will obtain

$$-\frac{d\{HF\}}{dt} = k_a[HF]^p \text{ ----- (S2.7)}$$

$$I_a = A_{Si}N_aFk_a[HF]^p \text{ ----- (S2.8)}$$

where k_a and p are constants, A_{Si} is the surface area of the silicon anode involved in the anodic reaction, N_a is the ratio of the number of moles of holes to the number of moles of HF consumed, which, according to the anodic reaction shown in the main text, is $1/2$. Since $I_c = I_a$ in the steady state,

$$s = G \frac{N_c}{N_a} \frac{k_c}{k_a} [H_2O_2]^m [HF]^{n-p} \text{----- (S2.9)}$$

where

$$G = \frac{A_{Au}}{A_{Si} / s} \text{----- (S2.10)}$$

s is the etch range of a static Au catalyst and G is the geometric parameter. With respect to Figure S1 and considering a single slice of the Au nanobeam of length dx (x-axis extends out of the page), it can be seen that for a given location under the Au catalyst, $A_{Si} = 2sdx$ (assuming that the anodic reaction takes place predominantly in the region of Si immediately adjacent to the Au catalyst) and $A_{Au} = (b + 2y) dx$. Since $t \ll b$, the contribution of t to A_{Au} is not taken into account here.

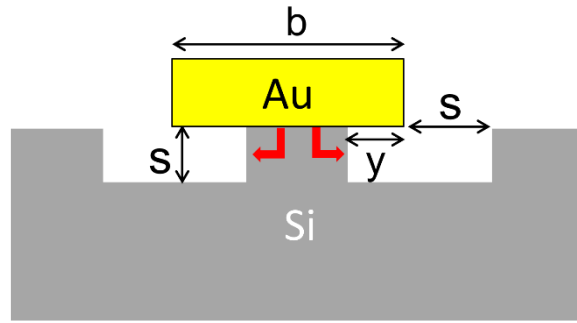


Figure S1: Schematic diagram showing MACE in process. Red arrows indicate the flow of h^+ from Au to Si.

Substituting A_{Si} and A_{Au} into eq. (S2.10) and (S2.9), it can be observed that s will vary with y as A_{Au} is a function of y . To simplify the model and subsequent calculations, we use an average A_{Au} which can be calculated in the following way:

$$\frac{1}{b/2} \int_0^b A_{Au} dy = \frac{3b}{2} dx \text{----- (S2.11)}$$

By using the average value of A_{Au} shown in eq. (S2.11), we can obtain an average value for s from eq. (S2.9) which is independent of y . The use of average values of A_{Au} and s in

subsequent calculations is not expected to introduce any significant error when we consider that the actual etching of Si during MACE is much more disorderly than that depicted in Figure S1. This is because the porous Si that forms underneath the metal catalyst as a result of this disorderly etching will have a roughness and thickness greater than the variation of s with y predicted by this model ($\sim 4\text{nm}$ or less)⁶. Therefore, any deviation between the predictions of this model and actual results is expected to be caused more by a lack of consideration for the formation of porous Si than the use of an average values for A_{Au} and s .

However, because the modelling for the formation of porous Si can be extremely involved, we will only focus on it in our future work. For now, the current model will suffice by providing a first order approximation of the relationship between s , $[\text{H}_2\text{O}_2]$ and $[\text{HF}]$. Evaluating eq. (S2.10), we will obtain $G = 3b/4$ for the Au nanobeams in eq. (S2.9) which can be also be expressed in the logarithmic form shown in eq. (3) in the main text.

Supporting Information 3: Computation of Hamaker constant, C

The Hamaker constant, C , in eq. (4) in the main text can be computed in the following way³:

$$C \approx (\sqrt{C_{Au}} - \sqrt{C_{sol}})(\sqrt{C_{Si}} - \sqrt{C_{sol}}) \text{----- (S3.1)}$$

where

$$C_{Au} \approx 4 \times 10^{-19}$$

$$C_{Si} = \frac{3}{4} kT \left(\frac{\varepsilon_{Si} - \varepsilon_0}{\varepsilon_{Si} + \varepsilon_0} \right)^2 + \frac{3h_0 \nu_e}{16\sqrt{2}} \frac{(n_{Si}^2 - n_0^2)^2}{(n_{Si}^2 + n_0^2)^{\frac{3}{2}}} \text{----- (S3.2)}$$

$$C_{sol} = \frac{3}{4} kT \left(\frac{\varepsilon_{sol} - \varepsilon_0}{\varepsilon_{sol} + \varepsilon_0} \right)^2 + \frac{3h_0 \nu_e}{16\sqrt{2}} \frac{(n_{sol}^2 - n_0^2)^2}{(n_{sol}^2 + n_0^2)^{\frac{3}{2}}} \text{----- (S3.3)}$$

k is the Boltzmann constant, T refers to the temperature ($\approx 300\text{K}$), h_0 refers to the Planck constant, ν_e refers to the mean absorption frequency ($\approx 3 \times 10^{15} \text{ Hz}^3$), ε and n refer to the dielectric constant and refractive index of the material indicated in the subscript. The subscripts Au, Si, sol and 0 refer to gold, silicon, etching solution (the optical properties of which can be approximated to be that of water⁷) and vacuum respectively. The values of the electromagnetic properties used for the various materials are summarized in Table S1. For Si-Au adhesion, C is found to be $2.76 \times 10^{-19} \text{ J}$ whereas for SiO_2 -Au adhesion, it is $2.54 \times 10^{-20} \text{ J}$.

	ε	n	$C(10^{-19}\text{J})$
Si	11.7 ⁸	3.4 ⁹	6.69
SiO₂	4.5 ¹⁰	1.5 ¹¹	0.62
Sol	83.3 ⁷	1.33 ¹²	0.37
0	1	1	-

Table S1: Summary of the optical values used and corresponding Hamaker constant obtained for each material.

Supporting Information 4: Derivation of expression for ν

To etch a single Si atom, QN_h amount of charges are required. Q refers to the charge an electron or hole carries ($=1.6 \times 10^{-19}\text{C}$) while N_h refers to the number of holes required to etch one Si atom which according to reaction (2) in the main text, is 3. Since the etch rate, ν , can give the number of Si atoms etched per unit time over a unit area, ν can be related to I_c ($=I_a$) with the following expression:

$$I_c = Av\chi QN_h \text{ ----- (S4.1)}$$

where A refers to the projected area over which the etching is taking place and χ refers to the density of Si atoms ($=5 \times 10^{28} / \text{m}^3$). Note that $Av\chi$ gives the number of Si atoms removed per unit time. Combining eq. (S4.1) with eq. (S2.6), we have

$$\nu = \frac{A_{Au}}{A} \frac{N_c F}{N_h \chi Q} k_c [H_2O_2]^m [HF]^n \text{ ----- (S4.2)}$$

which can be expressed in the logarithmic form shown in eq.(7) in the main text.

Derivation of ν for MACE using a metal film patterned with a square array of square holes

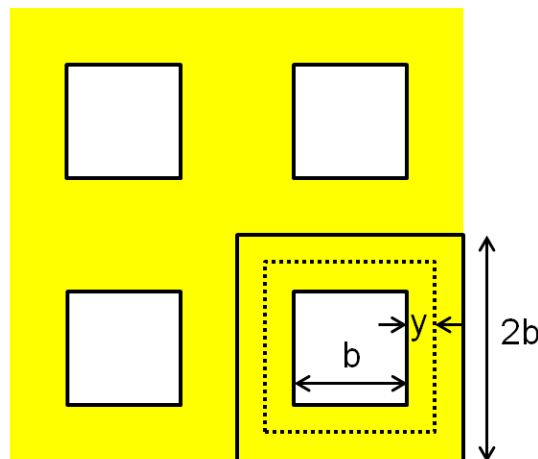


Figure S2: Schematic diagram showing the top view of a square array of square holes in a gold film.

Consider an Au film with a square array of square holes having a period of $2b$ and feature size b (Figure S2). When placed in the etching solution, the Si underneath the Au will

be removed, leaving nanopillars with cross-sectional areas of $b \times b$. During the etching process, the area of the Au film varies from $3b^2$ to $6b^2$ for each periodic feature as more and more of the underside of the Au film is exposed following the etching of Si. Substituting $A_{Au} = 2b^2 + (b+2y)^2$ in eq. (S2.11), we obtain an average value of $13b^2/3$ for A_{Au} in this case. Also, $A = (2b)^2 - b^2 = 3b^2$. Therefore, for an Au film with a square array of square holes of width b and period $2b$, $A_{Au}/A = 13/9$.

Supporting Information 5: Dependence of calculated σ with respect to estimation of L

From eq. (5) in the main text, the first order derivative of σ with respect to L can be written as

$$\frac{d\sigma}{dL} = -\frac{48E\psi\Delta z}{b} \frac{1}{x^2(L-x)^3} \text{ ----- (S5.1)}$$

From eq.(S6.1), it can be seen that for $x \rightarrow 0$ or $x \rightarrow L$, $d\sigma/dL \rightarrow \infty$. In contrast, for $x = L/2$, $d\sigma/dL$ has a finite value. This shows that the estimation of σ is significantly more sensitive to the estimation of L for points near the ends of the beam as compared to the center of the beam. Typically, for the samples in this study, 1% error in estimating L will bring about 3% or less error in estimating σ based on deflections in the center of the beam.

References

1. Avilés, F., Llanes, L. & Oliva, A. I. Elasto-plastic properties of gold thin films deposited onto polymeric substrates. *J. Mater. Sci.* **2009**, *44*, 2590–2598.
2. Pierret, R. F. *Semiconductor Device Fundamentals*. (Addison Wesley, 1996).
3. Israelachvili, J. N. *Intermolecular and Surface Forces, Second Edition: With Applications to Colloidal and Biological Systems*. (Academic Press, 1992).
4. LeVan, M. D. & Vermeulen, T. Binary Langmuir and Freundlich Isotherms for Ideal Adsorbed Solutions. *J. Phys. Chem.* **1981**, *85*, 3247–3250.
5. Connors, K. A. *Chemical Kinetics: The Study of Reaction Rates in Solution*. (John Wiley & Sons, 1990).
6. Geyer, N., Fuhrmann, B., Huang, Z., de Boor, J., Leipner, H. S. & Werner, P. Model for the Mass Transport during Metal-Assisted Chemical Etching with Contiguous Metal Films As Catalysts. *J. Phys. Chem. C* **2012**, *116*, 13446–13451.
7. Gross, P. M. & Taylor, R. C. The Dielectric Constants of Water, Hydrogen Peroxide and Hydrogen Peroxide—Water Mixtures. *J. Am. Chem. Soc.* **1950**, *72*, 2075–2080.
8. Dunlap, W. C. & Watters, R. L. Direct Measurement of the Dielectric Constants of Silicon and Germanium. *Phys. Rev.* **1953**, *92*, 1396–1397.
9. Li, H. H. Refractive Index of Silicon and Germanium and Its Wavelength and Temperature Derivatives. *J. Phys. Chem. Ref. Data* **1980**, *9*, 561–658.
10. Young, K. F. & Frederikse, H. P. R. Compilation of the Static Dielectric Constant of Inorganic Solids. *J. Phys. Chem. Ref. Data* **1973**, *2*, 313–410.
11. Pliskin, W. A. & Esch, R. P. Refractive Index of SiO₂ Films Grown on Silicon. *J. Appl. Phys.* **1965**, *36*, 2011–2013.

12. Schiebener, P., Straub, J., Levelt Sengers, J. M. H. & Gallagher, J. S. Refractive Index of Water and Steam as Function of Wavelength, Temperature and Density. *J. Phys. Chem. Ref. Data* **1990**, *19*, 677–717.